Influence of excitation and collection geometry on the dark field spectra of individual plasmonic nanostructures

Mark W. Knight,[1,2] Jonathan Fan,[3] Federico Capasso,[3] and Naomi J. Halas[1,2,*]

[1]*Department of Electrical and Computer Engineering, Rice University, Houston, Texas 77005, USA*
[2]*Laboratory for Nanophotonics, Rice University, Houston, Texas 77005, USA*
[3]*School of Engineering and Applied Sciences, Harvard University, Cambridge, Massachusetts 02138, USA*
[*]*halas@rice.edu*

Abstract: Dark field microspectroscopy is the primary method for the study of plasmon modes of individual metallic nanostructures. Light from a plasmonic nanostructure typically scatters with a strong angular and modal dependence, resulting in significant variations in the observed spectral response depending on excitation and collection angle and polarization of incident light. Here we examine how spectrally dependent radiation patterns arising from an individual plasmonic nanoparticle, positioned on a dielectric substrate, affect the detection of its plasmon modes. Careful consideration of excitation and collection geometry is of critical concern in quantitative studies of the optical response of these nanoparticle systems.

OCIS codes: (240.6680) Surface plasmons; (290.5820) Scattering measurements; (260.0260) Physical Optics; (240.3990) Micro-optical devices; (300.6650) Spectroscopy, visible.

References and links

1. S. Lal, S. Link, and N. J. Halas, "Nano-optics from sensing to waveguiding," Nat. Photonics **1**(11), 641–648 (2007).
2. L. Novotny, and B. Hecht, *Principles of nano-optics* (Cambridge University Press, Cambridge, 2006).
3. U. Kreibig, and M. Vollmer, *Optical properties of metal clusters* (Springer, Berlin, 1995).
4. P. Bharadwaj, B. Deutsch, and L. Novotny, "Optical antennas," Adv. Opt. Phot. **1**(3), 438–483 (2009).
5. M. Hu, C. Novo, A. Funston, H. Wang, H. Staleva, S. Zou, P. Mulvaney, Y. Xia, and G. V. Hartland, "Dark-field microscopy studies of single metal nanoparticles: understanding the factors that influence the linewidth of the localized surface plasmon resonance," J. Mater. Chem. **18**(17), 1949–1960 (2008).
6. C. L. Nehl, N. K. Grady, G. P. Goodrich, F. Tam, N. J. Halas, and J. H. Hafner, "Scattering spectra of single gold nanoshells," Nano Lett. **4**(12), 2355–2359 (2004).
7. S. Marhaba, G. Bachelier, C. Bonnet, M. Broyer, E. Cottancin, N. Grillet, J. Lermé, J.-L. Vialle, and M. Pellarin, "Surface plasmon resonance of single gold nanodimers near the conductive contact limit," J. Phys. Chem. C **113**(11), 4349–4356 (2009).
8. J. Zuloaga, E. Prodan, and P. Nordlander, "Quantum description of the plasmon resonances of a nanoparticle dimer," Nano Lett. **9**(2), 887–891 (2009).
9. C. Sönnichsen, S. Geier, N. Hecker, G. von Plessen, J. Feldmann, H. Ditlbacher, B. Lamprecht, J. Krenn, F. Aussenegg, V. Chan, J. Spatz, and M. Möller, "Spectroscopy of single metallic nanoparticles using total internal reflection microscopy," Appl. Phys. Lett. **77**(19), 2949–2951 (2000).
10. C. Sönnichsen, T. Franzl, T. Wilk, G. von Plessen, J. Feldmann, O. Wilson, and P. Mulvaney, "Drastic reduction of plasmon damping in gold nanorods," Phys. Rev. Lett. **88**(7), 077402 (2002).
11. J. J. Mock, M. Barbic, D. R. Smith, D. Schultz, and S. Schultz, "Shape effects in plasmon resonance of individual colloidal silver nanoparticles," J. Chem. Phys. **116**(15), 6755–6759 (2002).
12. J. J. Mock, D. R. Smith, and S. Schultz, "Local refractive index dependence of plasmon resonance spectra from individual nanoparticles," Nano Lett. **3**(4), 485–491 (2003).
13. S. Schultz, D. R. Smith, J. J. Mock, and D. A. Schultz, "Single-target molecule detection with nonbleaching multicolor optical immunolabels," Proc. Natl. Acad. Sci. U.S.A. **97**(3), 996–1001 (2000).
14. G. Schider, J. R. Krenn, A. Hohenau, H. Ditlbacher, A. Leitner, F. R. Aussenegg, W. L. Schaich, I. Puscasu, B. Monacelli, and G. Boreman, "Plasmon dispersion relation of Au and Ag nanowires," Phys. Rev. B **68**(15), 155427 (2003).
15. T. Søndergaard, and S. I. Bozhevolnyi, "Metal nano-strip optical resonators," Opt. Express **15**(7), 4198–4204 (2007).

#121585 - $15.00 USD Received 16 Dec 2009; revised 5 Jan 2010; accepted 11 Jan 2010; published 22 Jan 2010

16. M. W. Knight, Y. Wu, J. B. Lassiter, P. Nordlander, and N. J. Halas, "Substrates matter: influence of an adjacent dielectric on an individual plasmonic nanoparticle," Nano Lett. **9**(5), 2188–2192 (2009).
17. R. Ruppin, "Optical absorption of a coated sphere above a substrate," Physica A **178**(1), 195–205 (1991).
18. G. Videen, "Light scattering from a sphere on or near a surface," J. Opt. Soc. Am. A **8**(3), 483–489 (1991).
19. C. Beitia, Y. Borensztein, R. Lazzari, J. Nieto, and R. G. Barrera, "Substrate-induced multipolar resonances in supported free-electron metal spheres," Phys. Rev. B **60**(8), 6018–6022 (1999).
20. F. Moreno, F. González, and J. M. Saiz, "Plasmon spectroscopy of metallic nanoparticles above flat dielectric substrates," Opt. Lett. **31**(12), 1902–1904 (2006).
21. E. Eremina, Y. Eremin, and T. Wriedt, "Simulations of light scattering spectra of a nanoshell on plane interface based on the discrete sources method," Opt. Commun. **267**(2), 524–529 (2006).
22. S. J. Oldenburg, R. D. Averitt, S. L. Westcott, and N. J. Halas, "Nanoengineering of optical resonances," Chem. Phys. Lett. **288**(2-4), 243–247 (1998).
23. B. E. Brinson, J. B. Lassiter, C. S. Levin, R. Bardhan, N. Mirin, and N. J. Halas, "Nanoshells made easy: improving Au layer growth on nanoparticle surfaces," Langmuir **24**(24), 14166–14171 (2008).
24. P. B. Johnson, and R. W. Christy, "Optical constants of the noble metals," Phys. Rev. B **6**(12), 4370–4379 (1972).
25. J. Kvietkova, B. Daniel, M. Hetterich, M. Schubert, and D. Spemann, "Optical properties of ZnSe and $Zn_{0.87}Mn_{0.13}Se$ epilayers determined by spectroscopic ellipsometry," Thin Solid Films **455–456**, 228–230 (2004).
26. J. A. Stratton, *Electromagnetic theory* (McGraw-Hill, New York, 1941).
27. R. Juškaitis, "Characterizing high numerical aperture microscope objective lenses," in *Optical Imaging and Microscopy,* 2 ed., P. Török and F.-J. Kao, eds. (Springer, Berlin, 2007), pp. 21–43.
28. E. Prodan, C. Radloff, N. J. Halas, and P. Nordlander, "A hybridization model for the plasmon response of complex nanostructures," Science **302**(5644), 419–422 (2003).

1. Introduction

Nanoscale metallic structures, particles, and complexes interact strongly with light due to their collective electronic resonances, known as surface plasmons [1–4]. To study this class of systems requires methods that can probe the interaction between light and nanoscale structures with sufficient accuracy and detail to facilitate direct comparison between experimental data and theoretical models [5, 6]. As plasmonic nanostructures of increasing complexity are developed, some quite possibly with optical features beyond the classical electromagnetic limit [7, 8], the need for experimental tools to probe these systems accurately becomes critically important. Dark field microspectroscopy of individual nanostructures, where scattered light from an individual nanoparticle or nanocomplex is detected with spectral discrimination, currently provides a highly useful method to study, in detail, the plasmon modes of these systems [5, 9–13].

In dark field microspectroscopy, the scattered field emitted into the angular cone of the detection optics is frequently assumed to be representative of the total scattered field of the nanoscale complex. However, some plasmon modes may not radiate efficiently into the collection solid angle. This can result in significant deviations between the experimentally measured spectrum and theoretically calculated plasmon modes. The presence of a substrate may further alter the angular distribution of the scattered light from a nanoscale plasmonic system, in a mode-dependent manner.

In this study, we examine the role of the collection and excitation optics in the detection of plasmon modes from an individual plasmonic nanoparticle supported on a substrate. The system studied is a single Au nanoshell deposited on a substrate with a high dielectric constant (ZnSe). Previous studies have discussed the importance of the excitation angle [14, 15], and shown that the dielectric properties of a substrate can influence the properties of individual plasmonic nanoparticles supported on their surfaces quite significantly [16–21]. Here we present a systematic study of several factors that contribute to the relative amplitudes of the observed plasmon modes in experimental spectra: excitation angle of incident light, the numerical aperture (NA) of the collection optics, even small, local irregularities at the nanoparticle-substrate interface. These effects are generally applicable to the observation and characterization of the plasmon modes of metallic nanostructures, whether fabricated lithographically or by chemical means, and apply quite generally to the observations of plasmon modes of individual nanostructures or nanoparticles.

#121585 - $15.00 USD Received 16 Dec 2009; revised 5 Jan 2010; accepted 11 Jan 2010; published 22 Jan 2010

2. Methodology

2.1 Experimental sample preparation and measurements

Au nanoshells, spherical nanoparticles consisting of a dielectric core coated with a thin metallic shell, were synthesized as previously reported [22, 23]. The silica cores, obtained from Precision Colloid Inc., were measured to have an average radius of 62±5 nm using transmission electron microscopy (TEM). Nanoshells of dimensions $[r_1, r_2]$=[62, 95] nm, where r_1 corresponds to the core radius and r_2 corresponds to the total nanoshell radius, were fabricated. Polished ZnSe substrates were purchased from II-VI Infrared Inc. and patterned with gold markers structures to facilitate easy identification of specific individual particles for spectral and structural measurements of specific individual particles. Samples were prepared by drop-casting a dilute solution of nanoparticles, suspended in ethanol, onto the ZnSe substrate.

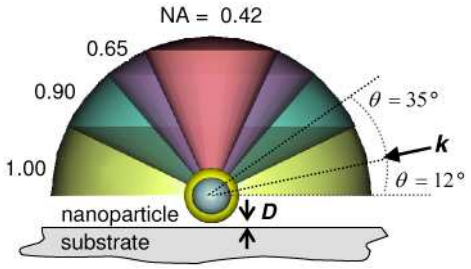

Fig. 1. Schematic of the nanoshell-substrate geometry. A dark-field objective collects light scattered by the nanoparticle, here an isolated Au-Silica nanoshell, separated from a dielectric substrate by a distance D, where $D < 0$ corresponds to a facet on the nanoparticle. Radiation cones corresponding to the numerical aperture of four common objectives are shown (NA = 0.42, 0.65, 0.90, and 1.00). Experimentally, the dark field geometry allows excitation over a narrow range of k vectors incident at an angle θ onto the substrate; in simulations the illumination is modeled as a monochromatic plane wave using the Fresnel equations to account for the presence of the substrate.

Single particle scattering spectroscopy was performed using a custom-built dark field microspectroscopy apparatus that allowed independent selection of the collection N.A. and excitation angle. Briefly, a halogen white light source was polarized with a broadband polarization cube, then focused onto the substrate at a particular incidence angle of $\theta = 12°$ or 35° (Fig. 1). Scattered light was collected using a Mitutoyo 50x IR-corrected objective with either NA = 0.42 or 0.65, dispersed in a Jobin Yvon grating spectrograph, and detected using a silicon CCD array detector. The light was imaged onto a pinhole to select scattering from a single nanoshell and suppress unwanted scattering from nearby, adjacent nanoparticles. The broadband spectral background was suppressed by subtracting the scattered light from a region of the substrate near the nanoshell from the raw particle spectrum. The final spectrum was corrected for the spectral efficiency of the entire microspectrometer by normalization with the scattering spectrum of a teflon white standard. Following optical characterization, the samples were coated with a ~5-10 nm thick PdPt film and imaged using a scanning electron microscope (SEM), where the nanoshells were identified using the gold marker pattern.

2.2 Simulations of single nanoparticle spectra

Spectra for a nanoshell supported on a dielectric substrate were calculated numerically using a commercially available FEM package (COMSOL Multiphysics 3.5, RF module). The nanoshell was modeled as two concentric spheres of radius r_1 and r_2 inside a spherical simulation space surrounded by perfectly matched layers (PMLs) and scattering boundary conditions to absorb scattered light. The refractive index of silica was used for the core (n = 1.42), with the shell layer of the nanoparticle defined using the empirically determined bulk dielectric function of gold [24].

#121585 - $15.00 USD Received 16 Dec 2009; revised 5 Jan 2010; accepted 11 Jan 2010; published 22 Jan 2010

The air/substrate boundary was defined as a plane offset from the particle origin by (r_2+D), where the distance D (Fig. 1) allows for either a gap between the particle and the substrate ($D > 0$), or the introduction of a flat 'facet' on the nanoparticle ($D < 0$). The substrate, in this work, was simulated using a constant refractive index of $n = 2.6$ to simplify interpretation of the results. The real dielectric function of ZnSe varies across the visible and NIR regions of the spectrum; however, for this system, spectra calculated using an empirical dielectric function for ZnSe [25] were extremely similar to calculations performed with a substrate with a constant dielectric. The similarity between these two approaches arises from the relatively small deviations in the magnitude of the screening charges induced on the dielectric surface as a function of wavelength. These charges are equivalent to an image of the induced charge on the nanoparticle reduced by a factor of (ε-1)/(ε+1) [2], a factor which does not vary significantly across the visible region of the spectrum for ZnSe.

The geometry, consisting of a single solitary particle adjacent to a substrate, is cylindrically symmetric. However, under plane wave excitation, the full electromagnetic solution has only a single mirror symmetry plane, defined by the k vector and the substrate normal. This symmetry plane was exploited in the simulations by specifying a boundary bisecting the simulation space and parallel to the k vector, and using either perfect electric conductor (PEC) or perfect magnetic conductor (PMC) boundary conditions for S and P polarized light, respectively. The use of symmetry reduced the number of degrees of freedom by half, to ~150K-300K. The finite collection angle associated with a given numerical aperture was included in the simulation by integrating the far-field scattering only over a semispherical boundary with an opening half angle of $sin^{-1}(\mathrm{NA})/n_{\mathrm{air}}$ (Fig. 1). The near-to-far field transform was performed using the Stratton-Chu formula [26]. More complex factors arising from the use of high numerical aperture objectives were neglected, such as apodization effects where collection efficiency can vary as a function of the angle of incidence and polarization of scattered light [27].

The particle was excited using a field satisfying the Fresnel equations for a plane wave incident at an angle θ above the substrate. This field definition, in the scattered field formulation, results in extremely low scattered field intensities far from the particle and allows a good approximation of an infinite substrate. In the case of an air ($n = 1$) substrate and a large numerical aperture, this approach yields normalized spectra identical to those calculated analytically using Mie theory.

3. Influence of numerical aperture and angle of excitation

3.1. Experimental spectra of nanoshells on a ZnSe substrate

Experimental spectra for nanoshells deposited on a ZnSe substrate exhibit two strong modes when excited with S-polarized light, along with a weaker, more redshifted mode for P-polarized excitation [16]. Briefly, a small nanoshell in a homogeneous medium has a single dipole resonance, since higher order resonances cannot be excited in the dipole limit. Finite size effects can allow higher order multipolar modes to be weakly excited, although the quadrupole plasmon appears only very weakly in the scattering spectrum even for a particle approaching 200 nm in diameter. When this particle is located adjacent to a substrate, the substrate reduces the symmetry of the system and lifts the threefold mode degeneracy associated with a symmetric particle in a uniform 3D medium. This effect can be understood using a simple image dipole picture, where the induced charge on the particle interacts with the induced image charges in the substrate. This reduction in symmetry results in hybridization between plasmon modes of different orders, leading to significantly redshifted mode energies and enhanced optical excitation of the quadrupolar plasmon mode. The dipolar mode splits into two separate modes, each associated with either a transverse or axial polarization of the electromagnetic field.

#121585 - $15.00 USD Received 16 Dec 2009; revised 5 Jan 2010; accepted 11 Jan 2010; published 22 Jan 2010

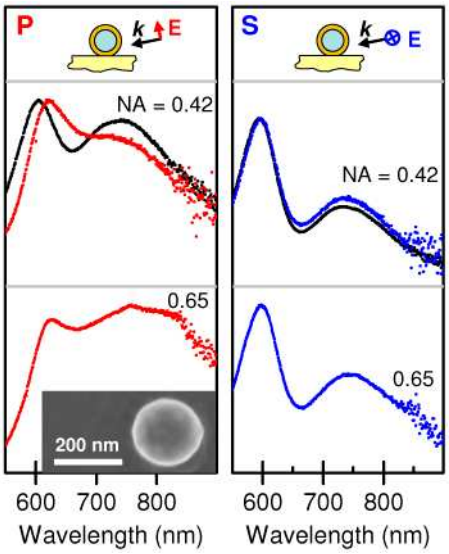

Fig. 2. Experimental spectra for an [r_1, r_2] ~[62, 95] nm nanoshell showing scattering spectra for P-polarized (red) and S-polarized (blue) incident light for two different objectives (NA = 0.42 and 0.65) and an excitation angle $\theta = 12°$. Spectra for an excitation angle of $\theta = 35°$ are also shown for a collection NA = 0.42 (black). Inset shows an SEM image of the nanoparticle corresponding to these spectra.

When investigating the properties of this system with darkfield microscopy, the numerical aperture of the objective has a strong effect on the amplitudes of the observed plasmon modes. This is shown in Fig. 2, where the P-polarized spectra (left) and S-polarized spectra (right) of the same individual nanoparticle are shown, for detection optics with two different numerical apertures. For P-polarized excitation, the amplitude of the quadrupolar mode (λ = 600 nm) decreases with increasing numerical aperture, relative to the dominant transverse dipolar mode (λ = 750 nm). The magnitude of this change is sensitive to local geometry of the particle and substrate. For some nanoparticles, a weak axial dipolar mode also becomes visible as a long wavelength shoulder at nominally 900 nm in the spectrum for the 0.65 NA objective. In contrast, for spectra obtained using S-polarized light, the peak amplitudes exhibit negligible variation due to changes in numerical aperture.

The amplitudes of the plasmon modes are also sensitive to excitation angle. When the same particle is excited with a higher incidence angle, $\theta = 35°$ rather than 12°, the spectrum for P-polarized light changes significantly (Fig. 2, black line). The spectral features become more resolved, and the transverse dipolar mode increases relative to the quadrupolar mode amplitude. For spectra obtained using S-polarized light, the peak amplitudes exhibit only very small changes as the excitation angle is varied.

While the spectra in Fig. 2 are normalized for clarity, changing the numerical aperture of the objective strongly affects the absolute intensity of the collected light. For example, substituting a 0.65 NA objective for a 0.42 NA objective more than doubles the absolute amplitude of the measured spectrum. (The higher noise levels for spectra collected with the 0.42 NA objective are evident in Fig. 2 above 850 nm in wavelength. Increasing the integration time on the CCD can partially compensate for the reduced signal associated with low NA objectives.)

Dark field measurements of faceted colloid with similar diameters to the nanoshells used here were performed with nearly identical results, as expected for nanoshells with thick shell layers, where plasmon hybridization affects the spectra only minimally [28].

#121585 - $15.00 USD Received 16 Dec 2009; revised 5 Jan 2010; accepted 11 Jan 2010; published 22 Jan 2010

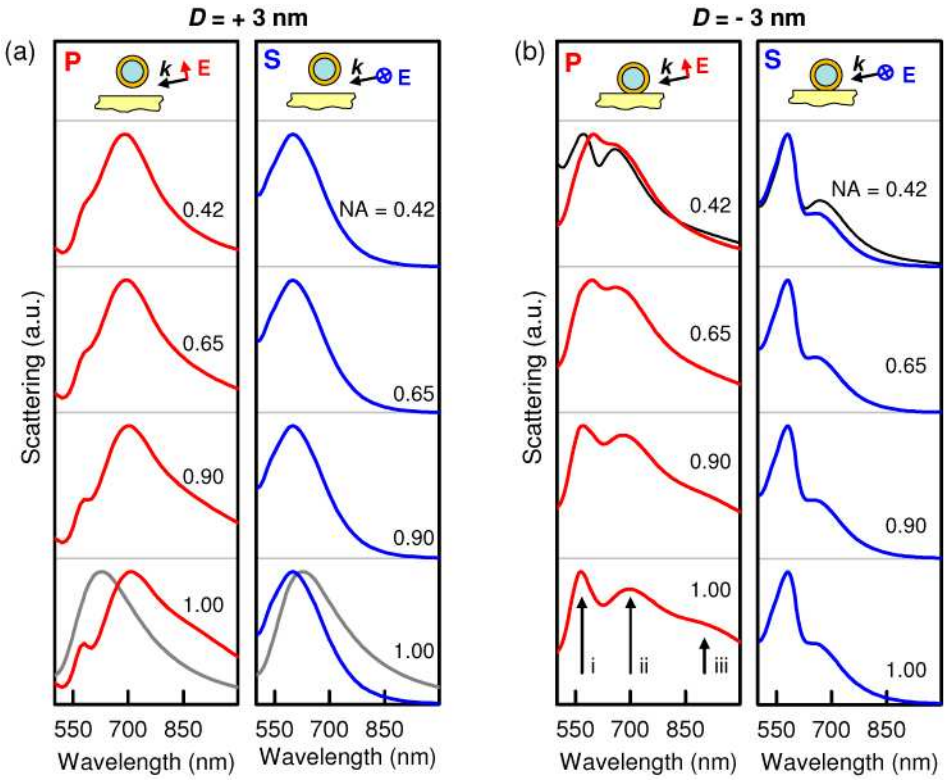

Fig. 3. Simulated spectra showing NA dependence for an [r_1, r_2] = [62, 95] nm nanoshell supported by a dielectric substrate (n = 2.6) for θ = 12° and polarization either perpendicular (P, red) or parallel (S, blue) to the substrate. The sensitive spectral dependence on gap geometry is illustrated with a nanoshell (a) separated from the substrate by a 3 nm gap, with Mie theory for the same nanoshell in air (gray), and (b) with a 3 nm facet (D = –3 nm) in contact with the substrate. (i) quadrupolar mode at 565 nm, (ii) transverse dipolar mode at 695 nm, and (iii) axial dipolar mode at 900 nm in wavelength. For NA = 0.42, excitation with θ = 35° is also shown (black lines). Spectra are normalized and offset for clarity.

3.2. Influence of nanoparticle-substrate geometry

In Fig. 3, simulations of the dark field spectroscopy of an individual nanoshell on a dielectric substrate with the same properties as our experimental system are shown. In this series of spectra, changes in the optical spectrum over a full range of NA values are investigated.

Independent of variations in numerical aperture, we observe a remarkably high sensitivity in the spectra depending on the local geometry of the nanoparticle at the nanoparticle-substrate interface. Spectra obtained for a spherical nanoparticle on a planar dielectric substrate (Fig. 3, left) do not resemble, even qualitatively, the spectra of our system (Fig. 2). However, by introducing a very small degree of nanoparticle flattening (D = –3 nm) at the nanoparticle-ZnSe substrate interface, we obtain very good agreement between simulated spectra (Fig. 3, right) and the observed experimental spectra (Fig. 2). Such a small deformation, less than a 2% deviation in nanoparticle diameter, may easily result from faceting of the multicrystalline shell layer of the nanoparticle (Fig. 2, inset). A similar series of spectra are obtained for a spherical nanoparticle on a dielectric substrate with a small equivalent (3 nm) indentation. The presence of a nanometer scale facet or depression at the nanoparticle-substrate interface induces a redshifting of the transverse dipolar mode, and an increase in the quadrupole mode amplitude from a weak spectral shoulder to the dominant peak in the spectrum. Also, the axial dipolar mode at 850 nm strengthens significantly. In general, the spectra are highly sensitive to the depth of this facet or deformation, which suggests that nanoparticle-to-nanoparticle variability in the scattering spectrum may be due to

#121585 - $15.00 USD Received 16 Dec 2009; revised 5 Jan 2010; accepted 11 Jan 2010; published 22 Jan 2010

these small structural variations. Interparticle spectral variation may be minimized by introducing an index-matching oil to reduce the effect of the interface [12].

3.3. Influence of numerical aperture on scattering spectra

The numerical aperture of the collection objective can significantly modify the mode amplitudes of the experimentally observed spectrum. In Fig. 3, a series of spectra show the amplitude of the axial dipolar mode (λ = 900 nm) steadily increasing with increasing numerical aperture for P-polarized excitation, with the quadrupolar (λ = 565 nm) and transverse dipolar (λ = 695 nm) peaks becoming increasingly spectrally resolved. This same increase in numerical aperture induces a negligible effect on the S-polarized spectrum.

These trends arise from the radiation pattern associated with each plasmon mode. In Fig. 4, we examine the angular scattering distribution of each mode, within the solid collection angles corresponding to each numerical aperture studied. For P polarized light, the quadrupolar mode at 565 nm and the transverse dipolar mode at 695 nm both scatter light vertically toward the objective, while the axial dipolar mode at 900 nm radiates at a small angle above the substrate (Fig. 4(a)). Low NA objectives do not capture the scattered radiation from the axial dipolar mode, resulting in the absence of this mode in low NA spectra when that mode is excited. For S-polarized excitation (Fig. 4(b)), the apparent insensitivity to objective NA results from the quadrupolar (565 nm) and transverse dipolar (695 nm) modes radiating toward the objective in an extremely similar manner. For this polarization, increasing the numerical aperture increases the overall amplitude of the spectrum, but does not significantly modify the relative peak heights of the spectra.

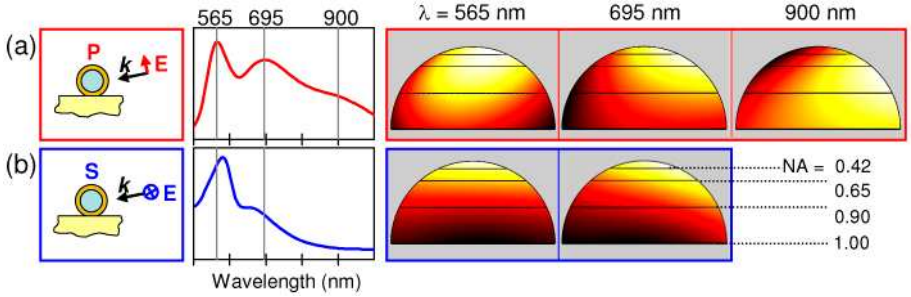

Fig. 4. Scattering spectra and radiation patterns for a [r_1, r_2] = [62, 95] nm nanoshell with a 3 nm facet supported on a substrate (n = 2.6) and either (a) P-polarized or (b) S-polarized excitation. Radiation diagrams show the far-field radiation on a hemispherical surface centered on the nanoparticle (normalized for clarity), with horizontal lines indicating the lower integration boundary for each simulated NA.

3.4. Influence of excitation angle on simulated spectra

The relative intensities of the plasmon modes in the scattering spectra also exhibit a sensitive dependence on excitation angle (Fig. 2). This dependence is examined in a series of simulations of single nanoparticle spectra for an excitation angle θ = 5° to 55°, where the numerical aperture of the collection optics is maintained at a constant value (Fig. 5).

The scattered light spectrum for P-polarized excitation depends critically on excitation angle. The axial dipolar mode is strongly excited only at low angles of incidence. Even when excited, however, this mode only appears in the spectra when large NA objectives are used in the collection optics (Fig. 5(a)). The quadrupole mode also shows a significant change in peak amplitude as the excitation angle is changed; this behavior was observed experimentally (Fig. 2). In our series of simulations, we observe that the range of excitation angles where the quadrupole mode is smallest occurs in the vicinity of Brewster's angle (θ = 21°), where reflections from the substrate are minimal and the particle is therefore excited with a more homogeneous field. We find that this behavior occurs for both small and large NA in P polarization (Fig. 5(a)).

#121585 - $15.00 USD Received 16 Dec 2009; revised 5 Jan 2010; accepted 11 Jan 2010; published 22 Jan 2010

In the case of S polarized excitation, the amplitude of the transverse dipolar mode gradually increases relative to the quadrupolar mode with increasing excitation angle (Fig. 5(b)). Only spectra for one NA (0.42) are shown for S polarization, since changing the numerical aperture of the objective did not result in significant modifications of the peak amplitudes (Fig. 3). For larger excitation angles, the quadrupolar mode recovers and, as required by symmetry, the S and P polarized spectra begin to converge.

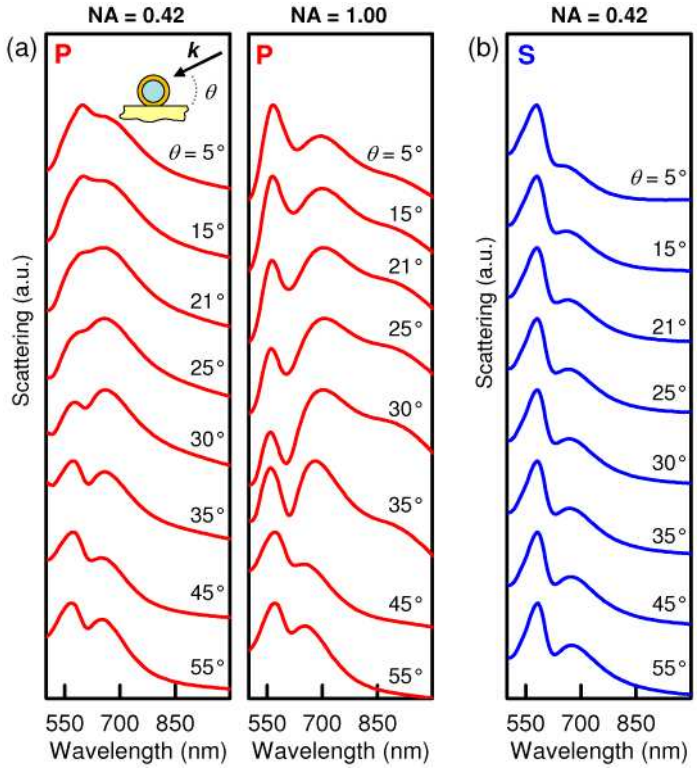

Fig. 5. Simulated spectra for a [62, 95] nm nanoshell with $D = -3$ nm showing the effect of incidence angle for (a) p polarized light for NA = 0.42 and 1.00 and (b) s polarized light for NA = 0.42. Spectra are normalized for clarity.

5. Summary

Experimental scattering spectra of individual plasmonic nanostructures depend sensitively on excitation and collection angles, and may not be equivalent to a complete spectrum including all scattered light. We have shown here, both experimentally and in simulations, that the numerical aperture of the collection objective significantly affects the spectra of a supported nanoshell, where the interaction with the dielectric substrate gives rise to multimode behavior. More generally, a restricted collection angle can influence the spectra of all complex plasmonic structures, even in homogeneous media, due to an unequal sampling of radiation from multiple modes [5]. As a result, even spectra collected using immersion oil may be modified by the limited collection angle of the objective.

With the increasing technological significance of nanoscale plasmonic structures, and the corresponding importance of accurate single structure characterization, understanding the effects of excitation and collection optics on the dark field spectra of these systems becomes increasingly important. However, while spectral peak amplitudes may be sensitive to experimental geometry, the mode energies themselves are an intrinsic property of the nanoscale system. Given an objective capable of sampling scattered light from all modes of

#121585 - $15.00 USD Received 16 Dec 2009; revised 5 Jan 2010; accepted 11 Jan 2010; published 22 Jan 2010

interest, dark field microscopy offers a robust method for probing the plasmonic properties of individual nanostructures.

Acknowledgements

We thank Peter Nordlander, J. Britt Lassiter, Nathaniel K. Grady and Surbhi Lal for insightful discussions on this subject. This material is based upon work supported as part of the Center for Advanced Solar Photophysics, an Energy Frontier Research Center funded by the U.S. Department of Energy, Office of Science, Office of Basic Energy Sciences. This work was supported by the NSF IGERT (M.W.K). (DG-0504425), the Robert A. Welch Foundation under Grant C-1220 (N.J.H.), and the DoD NSSEFF (NJH). J.F. and F.C. acknowledge funding by the NSF NIRT under Grant No. 0709323. Electron microscopy was performed at the Center for Nanoscale Science (CNS) at Harvard University. CNS is a member of the National Nanotechnology Infrastructure Network.

#121585 - $15.00 USD Received 16 Dec 2009; revised 5 Jan 2010; accepted 11 Jan 2010; published 22 Jan 2010